

Article

Improving Nanofiber Membrane Characteristics and Membrane Distillation Performance of Heat-Pressed Membranes via Annealing Post-Treatment

Minwei Yao, Yun Chul Woo, Leonard D. Tijing ^{*}, Cecilia Cesarini and Ho Kyong Shon ^{*}

Centre for Technology in Water and Wastewater, School of Civil and Environmental Engineering, University of Technology Sydney (UTS), 15 Broadway, Ultimo NSW 2007, Australia; minwei.yao@student.uts.edu.au (M.Y.); Yunchul.Woo@student.uts.edu.au (Y.C.W.); Cecilia.Cesarini@uts.edu.au (C.C.)

^{*} Correspondence: Leonard.Tijing@uts.edu.au (L.D.T.); Hokyong.Shon-1@uts.edu.au (H.K.S.);
Tel.: +61-2-9514-2652 (L.D.T.); +61-2-9514-2629 (H.K.S.)

Academic Editor: Enrico Drioli

Received: 16 December 2016; Accepted: 5 January 2017; Published: 12 January 2017

Abstract: Electrospun membranes are gaining interest for use in membrane distillation (MD) due to their high porosity and interconnected pore structure; however, they are still susceptible to wetting during MD operation because of their relatively low liquid entry pressure (LEP). In this study, post-treatment had been applied to improve the LEP, as well as its permeation and salt rejection efficiency. The post-treatment included two continuous procedures: heat-pressing and annealing. In this study, annealing was applied on the membranes that had been heat-pressed. It was found that annealing improved the MD performance as the average flux reached 35 L/m²·h or LMH (>10% improvement of the ones without annealing) while still maintaining 99.99% salt rejection. Further tests on LEP, contact angle, and pore size distribution explain the improvement due to annealing well. Fourier transform infrared spectroscopy and X-ray diffraction analyses of the membranes showed that there was an increase in the crystallinity of the polyvinylidene fluoride-co-hexafluoropropylene (PVDF-HFP) membrane; also, peaks indicating the α phase of polyvinylidene fluoride (PVDF) became noticeable after annealing, indicating some β and amorphous states of polymer were converted into the α phase. The changes were favorable for membrane distillation as the non-polar α phase of PVDF reduces the dipolar attraction force between the membrane and water molecules, and the increase in crystallinity would result in higher thermal stability. The present results indicate the positive effect of the heat-press followed by an annealing post-treatment on the membrane characteristics and MD performance.

Keywords: membrane distillation; post-treatment; annealing; PVDF-HFP; crystallinity

1. Introduction

The shortage of water is one of the biggest concerns for future society as the human population is increasing steadily. Desalination, a good option for coastal areas short of fresh water, has been becoming the major approach for potable water as the supply of seawater can be considered unlimited. Presently, reverse osmosis (RO) has reached the state of the art and has become the dominant technology because of its higher energy efficiency and stability compared to conventional thermal-based processes [1]. However, there are two main issues in RO: high energy consumption and brine treatment, which are becoming great challenges for future human society [2]. Hence, continuous efforts for finding new technologies that can provide lower energy consumption while still obtaining high process and production efficiencies are being sought out [3]. Among them, membrane distillation (MD) is one of the most promising emerging technologies [4].

One of the major advantages for MD is the potential usage of low-grade waste heat as its feed temperature requirement is much lower than that of the conventional distillation process. If sufficient waste heat is available, much less energy will be required for operation. Fundamentally, the membranes in MD serve as contactors, and are not involved in the separation process themselves. The mass transport starts from the evaporation of water at the boundary between the vapor and liquid phase at the membrane pores. Then the vapor is driven by the partial pressure, caused by a partial vapor pressure difference which is triggered by the temperature difference between the hot feed and cold permeate [5,6].

Although MD has these unique advantages, major challenges must still be addressed for its wide acceptance in the industry, which include a lack of specifically designed MD membranes and modules, difficulty in up-scaling the laboratory setup, and a shortage of techno-economic data [6]. Membrane fabrication has gained a great deal of interest, as researchers are using membranes designed for other processes. However, the characteristics of a decent MD membrane are different, as much higher hydrophobicity and liquid entry pressure (LEP) with high porosity are needed for a high flux performance with minimal wetting issues [7]. Polymers with relatively lower surface energies, such as polystyrene, polyvinylidene and polytetrafluoroethylene, have been used to fabricate membranes in the laboratory [8–11]. Phase inversion is one of the most used techniques due to its simplicity [12,13]. However, its products usually have low flux in MD due to its relatively low porosity and pore size [14,15].

Currently, electrospinning is gaining popularity in membrane fabrication [8–10,13,16]. Electrospun membranes have many advantages including a high contact angle, very high porosity, and simplicity for modification, making them very suitable for MD [17,18]. However, they have a large maximum pore size and, hence, a low LEP, making them susceptible to wetting [6,18]. Much effort has been invested into finding solutions to improve their LEP. For example, Prince fabricated a modified electrospun membrane by adding lab-made macromolecules into the solution, and later made a composite membrane consisting of both electrospun and phase inversion membranes, improving its LEP enormously [13,19]. Liao improved the LEP by adding surface-modified silica nanoparticles into the solution [16]. Lee added fluorosilane-coated TiO₂ into the solution and obtained an electrospun membrane with an increased LEP [20]. Other hydrophobic nanoparticles used as additives, including graphene and carbon nanotubes, were also extensively studied [12,21]. The other method is to incorporate a secondary polymer with very low surface tension into the polymer solution. Polydimethylsiloxane (PDMS) was found to be able to improve the hydrophobicity and LEP when mixed with the carrier polymer in the solution [22,23].

Post-modification techniques such as heat-pressing have been studied to improve the characteristics and membrane distillation performance of the electrospun membranes [24,25]. In our previous study, the effects of heat-press conditions were fully studied [24]. It was found that the temperature and duration played more important roles than pressure during heat-pressing. The properties of the electrospun membrane were impressively improved by heat-pressing. Although the contact angle and porosity decreased, the LEP and, hence, permeation performance in desalination improved greatly. In this study, to further improve the properties of the electrospun membranes, annealing, a commonly practiced thermal treatment, was applied to the heat-pressed membrane. A favorable change of the properties was achieved, and the MD performance was further improved.

2. Materials and Methods

2.1. Materials

Polyvinylidene fluoride-co-hexafluoropropylene (referred herein as PVDF-HFP, MW = 455,000) was purchased from Sigma-Aldrich, Sheboygan, WI, USA. For membrane fabrication, acetone (ChemSupply, Adelaide, Australia) and N,N-Dimethylacetamide (DMAc, Sigma-Aldrich, Sheboygan, WI, USA) were utilized as solvents. All the chemicals were used as received without further purification. A polypropylene (PP) filter layer purchased from Ahlstrom (Helsinki, Finland) was applied as support layer in all the MD tests except when commercial membrane was in use. Commercial microfiltration

membrane (pore size = 0.22 μm , porosity = 70%, GVHP) bought from Millipore (Jaffrey, NH, USA) was tested for comparison.

2.2. Membrane Fabrication by Electrospinning

PVDF-HFP (20 wt. %) was dissolved in a composite solvent comprising acetone and DMAc (1:4 acetone/DMAc ratio). The polymer powder was added into the mixed solvent and stirred by magnetic stirrer for 24 h at room temperature for complete dissolution. During electrospinning process, a 6 mL volume of the polymer solution was electrospun at a rate of 1 mL/h by applying 21 kV voltage between the tip of the spinneret and the rotating collector (metal drum) with a tip-to-collector distance of 20 cm. The relative humidity of the process chamber during electrospinning was in the range of 46%–54% at room temperature.

2.3. Post-Treatment of Electrospun Membranes

After the completion of the electrospinning, the just-fabricated membranes were removed from the collector and dried at 50 $^{\circ}\text{C}$ for 2 h inside an air flow oven (OTWMHD24, Labec, Sydney, Australia). The membranes were then heat-pressed by being set between flat metal plates with dead weight (6.5 kPa) placed on the top plate in a pre-heated oven at temperature of 150 $^{\circ}\text{C}$, while fully covered by foils. A 24 h heat-pressing was implemented for thorough microstructure evolution.

After heat-pressing, membrane annealing was realized by removing the dead weight on the membranes and leaving the pressed membranes in the oven at 120 $^{\circ}\text{C}$ (where temperature had been gradually decreased by 10 $^{\circ}\text{C}$ per hour from 150 $^{\circ}\text{C}$) for another one to three days. After these day(s), the membranes were slowly cooled by reducing temperature in the oven by 10 $^{\circ}\text{C}$ per hour, until room temperature was reached. The samples were named in Table 1 as shown below.

Table 1. Sample names and thicknesses of the membranes prepared in the present study.

Sample Name	Description	Membrane Thickness (μm)
Neat	As-spun electrospun PVDF-HFP (polyvinylidene fluoride-co-hexafluoropropylene) membranes	51
HP	Neat membrane heat-pressed at 150 $^{\circ}\text{C}$ under 6.5 kPa for 24 h	39
A1	HP membranes annealed for 1 day at 120 $^{\circ}\text{C}$	37
A2	HP membranes annealed for 2 days at 120 $^{\circ}\text{C}$	34
A3	HP membranes annealed for 3 days at 120 $^{\circ}\text{C}$	34

2.4. Characterization

Contact angle, which was generally used to indicate hydrophobicity of membrane surface, was measured by Theta Lite 100 (Attension) (Biolin Scientific, Paramus, NJ, USA) with sessile drop method [24,26]. Then 5–8 μL of water droplet was placed onto the membrane surface for analysis. A mounted motion camera was applied to capture the images at a rate of 12 frames per second. Contact angle could be obtained by analyzing the recorded video with aid of the Attension software. An average of three values was used as contact angle data for each sample.

As-spun, heat-pressed and annealed membrane samples was measured with a lab-made setup for their liquid entry pressure [9,24]. A gas supply was connected to a hollow stainless plate by a tube, with a digital gauge standing as the intermediate between them. On the top of the stainless plate, a stainless cylinder container was fully filled with distilled water while a plastic plug stuck in its bottom. The samples were firmly fixed on the top of cylinder by a stainless cap with a lock catch. The nitrogen gas was steadily released to increase the pressure by 5 kPa per 30 s, until the first bubble sign appeared, which was recorded as LEP. Each sample was tested in triplicate and average data was recorded.

Fourier-transform infrared (FT-IR) spectroscopy (Varian 2000, Agilent, Santa Clara, CA, USA) was used to investigate the PVDF-HFP phases of the virgin membrane and thermally-treated membranes. Each spectrum was acquired with signal averaging 32 scans at a resolution of 8 cm^{-1} , in transfer mode by pressing the sample with KBr to a pellet.

X-ray diffraction (XRD) (Siemens D5000, Siemens, Karlsruhe, Germany) was carried out over Bragg angles ranging from 10° to 30° (Cu K α , $\lambda = 1.54059 \text{ \AA}$).

The pore size and pore size distribution of the fabricated neat and post-treated electrospun membranes were measured by capillary flow porometry (CFP-1200-AEXL, Porous materials Inc., Ithaca, NY, USA). All samples were firstly wetted by Galwick (a wetting liquid with a low surface tension of 15.9 dynes/cm) and tested under the pre-set conditions. Then the dried samples were applied with N₂ gas to determine the gas permeability under same conditions. The final average pore size and its distribution were automatically calculated with both data sets of wet and dry tests by the specific software.

Membrane porosity was calculated by using gravimetric method, where the volume of the membrane pores was divided by the total volume of the whole membrane. Ethanol (Univar 1170 from Ajax Finechem Pty Ltd., Sydney, Australia) was used to completely wet the membranes. The weight (w_1 , g) of wetted membrane was measured after the residual ethanol on the surface was removed. Then the membrane samples were dried after being left still in the open air for 15 min and then weighed (w_2 , g). The porosity of the electrospun membranes could be calculated with the following equation:

$$\epsilon_m = \frac{(w_1 - w_2) / \rho_e}{(w_1 - w_2) / \rho_e + w_2 / \rho_p}$$

where ρ_e is the density of the ethanol (g/m³) and ρ_p is the density of the PVDF-HFP (g/m³) [16,24].

2.5. Direct Contact Membrane Distillation (DCMD) Test

MD has several common configurations: direct contact MD (DCMD), air gap MD (AGMD), vacuum MD (VMD), and sweeping gas MD (SGMD) [2]. Recently, permeate gap MD (PGMD) is gaining lots of interests due to its simple configuration [6], this study was focused on DCMD configuration, which is illustrated in Figure 1. Supported by a PP filter layer, the membrane samples were fixed in the DCMD cell module with a length and width of 77 mm and 26 mm, respectively, making up an effective membrane area of 20 cm², for both feed and permeate channels. The module was placed horizontally and ran in counter-current mode with feed flow on top side [9]. Sodium chloride (NaCl) (3.5 wt. % concentration) was used as feed, and deionized (DI) water was used as permeate, with temperature maintained at 60 °C and 20 °C, respectively. The mass flow rates of 400 mL/min were maintained by gear pumps for both feed and permeate flows. A desktop computer was used to collect the data of mass of permeate tank and temperatures in both feed and permeate tanks automatically. Permeation performances (flux and salt rejection) of post-treated electrospun membranes were compared with a commercial membrane (GVHP, 0.22 pore size, and 110 μm thickness).

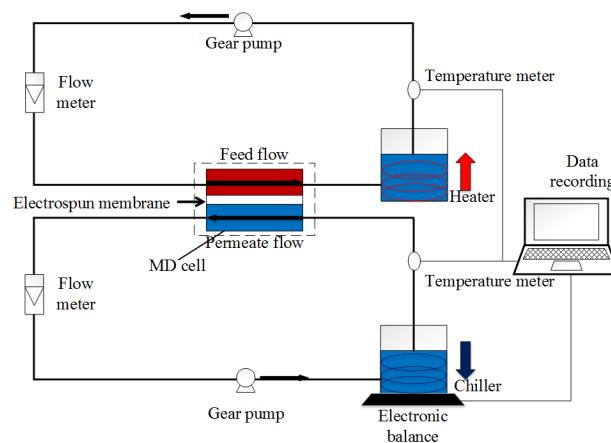


Figure 1. Schematic figure of DCMD (direct contact membrane distillation) system used in this study.

3. Results and Discussion

3.1. DCMD Performance

All the heat-pressed and annealed membranes had a salt rejection of 99.99%, while the neat membrane suffered rapid wetting immediately 30 s after the operation started. The wetting of electrospun membranes could be judged based on the steady increase in the flux and the conductivity of the permeate (exceeding 10 mS/cm). Figure 2 shows that optimal heat-pressing improves the flux and wetting resistance. An average of 28.7 LMH was obtained during 10 h of operation, which is much higher than in previous studies under similar conditions. For comparison, Liao et al. achieved a flux of 20.6 LMH with heat-pressed electrospun nanofiber membranes in DCMD [27]. Another study obtained a flux of 22 LMH with heat-pressed, two-layer membranes where the PVDF-HFP concentration was 10% [28]. However, the heat-pressed electrospun nanofiber membrane in the present study still has a noticeable decreasing trend during the 10 h of operation. On the other hand, annealed membranes showed a noticeably higher flux than the heat-pressed membrane, although they shared a close membrane thickness (Figure 2). Moreover, the annealed membrane showed a more stable trend of flux in 10 h of operation than HP, indicating a better wetting resistance. The membrane annealed for two and three days shared a similar performance, and both of them performed better than the membrane annealed for one day. The flux of the commercial membrane (GVHP) is illustrated here for comparison. A2 and A3, having a superb average flux of 35 LMH in 10 h of operation, were 75% higher than GVHP (20 LMH).

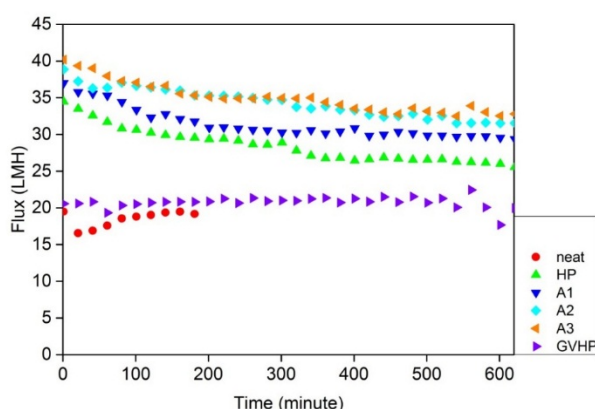


Figure 2. Comparison of flux performance between post-treated and as-spun electrospun membranes and commercial ones.

3.2. Increased Crystallinity and Appearance of α Phase after Annealing

FT-IR spectra of the α and β phases of PVDF in the PVDF-HFP copolymer were investigated comprehensively. It was found that the bands in terms of the β phase of PVDF appeared at 840 cm^{-1} and 1278 cm^{-1} [29,30] in all the as-spun and thermal-treated membranes, as shown in Figure 3; the bands related to the α phase of PVDF appeared at 615 cm^{-1} , 765 cm^{-1} , 795 cm^{-1} , 975 cm^{-1} and 1212 cm^{-1} [29–31], and they were only found in the annealed membranes. The phase of PVDF in the neat membrane was basically β , as the peak representing the α phase rarely appeared. Two factors contributed to the as-spun membranes mainly consisting of the β phase: (1) the existence of the HFP copolymer in the polymer chains [29]; (2) stretching and pulling of the electrospun fiber during the whipping process in electrospinning [31,32]. After the neat membrane was heat-pressed, the band at 840 cm^{-1} representing the β phase increased from 53% to 63.6%, while the band in terms of the α phase did not appear after the heat-press treatment. The increase in the transmittance of β phase bands indicated the increase in the crystallinity of the membrane as the amorphous phase of the PVDF was converted into the β phase due to the mechanical deformation, caused by the pressure

applied on the membranes during heat-pressing [25,26]. Vineet et al. found that annealing PVDF above 80° led to an increase in both the total crystallinity and the α phase PVDF percentage [29,33]. Du et al. also pointed out that annealing of the membrane resulted in the transformation of some regions of the PVDF phase from β to α [29]. In this study, bands in terms of the α phase started to appear at 615 cm^{-1} , 765 cm^{-1} , and 975 cm^{-1} after one day of annealing (A1), and were more obvious at 615 cm^{-1} , 765 cm^{-1} , 795 cm^{-1} , 975 cm^{-1} and 1212 cm^{-1} after two and three days of annealing (A2 and A3), while the transmittance at the 840 cm^{-1} band decreased back to 62.1% which is same value as in the neat membrane. It is worth noting that the membrane annealed for three days (A3) had nearly identical FT-IR spectra results as the one annealed for two days (A2), which means two days of annealing could be long enough for sufficient state conversion. The appearance of the α phase PVDF in the membrane is favorable for the MD process owing to its non-polar properties because it leads to a decrease in the dipolar interaction between the water molecules and the membrane [34]. The existence of the α phase PVDF can increase the liquid entry pressure and, hence, the wetting resistance, contributing to better long-term MD performance. Saffarini et al. stated that annealing could also affect the microstructure evolution [35], which benefits the long-term MD operation as well. By increasing the crystallinity and releasing the internal stresses caused by the heat-pressing, the thermal stability of the membrane could be improved, preventing the LEP from dropping rapidly owing to distortion at a high feed temperature.

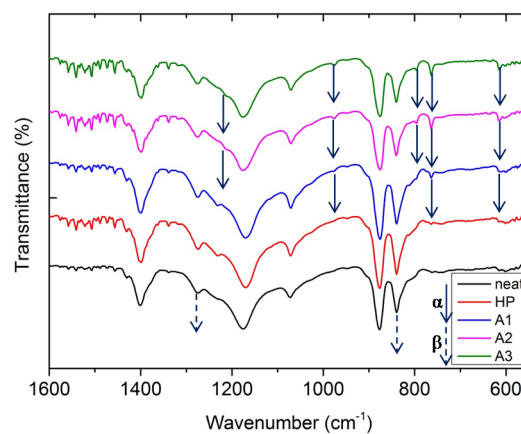


Figure 3. FT-IR (Fourier-transform infrared) spectra of as-spun and thermal -treated electrospun membranes.

3.3. Further Detection of Phase Conversion by XRD

To further confirm the change of the PVDF crystal phase in the PVDF-HFP membranes, X-ray diffraction was conducted on these membrane samples. Figure 4 shows the amorphous and both the α and β crystalline phases of PVDF in the PVDF-HFP electrospun membranes with or without post-treatment. It can be clearly seen that the as-spun electrospun membrane has many more regions containing the amorphous phase of PVDF as the peaks representing the α and β phases have been merged, leading to a much broader and weaker peak. It is worth noting that the amorphous state of the PVDF cannot be detected by FT-IR as discussed in last section. After heat treatment, the regions of the amorphous-state PVDF reduced greatly as two sharp peaks at 18.4° and 20.8° appeared, representing α (020) and β (110), respectively [29,30]. The sharp increase in the crystallinity of the PVDF-HFP membrane resulted in a great change of the membrane properties, especially the contact angle and LEP, which will be discussed in later sections. Annealing of the heat-pressed membrane can further improve the crystalline structure of the PVDF-HFP membrane in a favorable way. Due to the non-polar structure, the membrane composed of more regions of the α -phase PVDF had higher hydrophobicity, leading to a higher wetting resistance. While the total crystallinity maintained was nearly unchanged,

annealing the heat-pressed membrane for one day at 120 °C could convert the β phase to the α phase as the relative peaks varied. After the membranes were further annealed for another day, both the α phase and crystallinity were increased, leading to the increase in the thermal and mechanical stability [30]. More interestingly, a sharp new peak with a high intensity at 28.1° appeared, which is very close to α (111) having a two-theta angle of 27.8°. Considering the various new peaks representing the α phase PVDF crystal appearing in the FT-IR in the A2 membranes, we assumed that the peak at the 2θ angle of 28.1° was α (111) [30,32]. The high intensity of α (111) means a big increase in the α phase PVDF as well as the total crystallinity, so we believe that more amorphous phase of the PVDF along with the β phase was converted to the α phase. A3 (the membrane annealed for three days) shows identical spectra of XRD results as A2, so it is not shown in Figure 4.

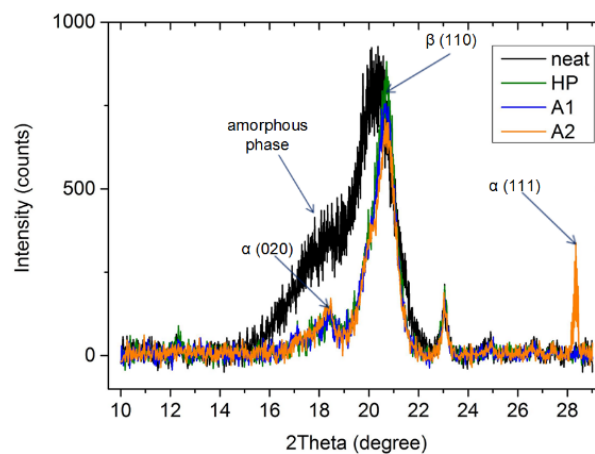


Figure 4. XRD (X-ray diffraction) patterns (2θ spectra) of as-spun and thermal-treated electrospun membranes.

3.4. Improvement of Membrane Properties

3.4.1. Pore Size Distribution and Porosity

Figure 5 shows the pore size distribution of membranes before and after the heat treatment. The as-spun membrane has an average pore diameter of 1.3 μm and a much wider range (from 0.8 μm to 2.2 μm) than the other samples. The heat-pressed membrane (HP) has the smallest average pore size (1.1 μm) and a much smaller range of the pore diameter compared with the neat membranes because the fibers were deformed and widened under high pressure at 150 °C [24]. Annealing the HP membranes for one day can further narrow the pore size distribution, although the mean pore diameter increased slightly from 1.1 μm to 1.2 μm . The increase in the average pore size may be due to the further decrease in the membrane thickness from 39 μm to 37 μm , which might be caused by the release of internal stress generated during heat-pressing; the other possible cause could be the supplementary merging of the crystalline phase of the PVDF which was converted from the amorphous phase during annealing [30]. The results were consistent with the study of Saffarini et al., as it was found that an increase in the annealing temperature would lead to an increase in the average pore size of the membranes [35]. Further annealing for another day led to a greater decrease in the range of the pore diameter and a sharp peak appeared, although the average mean pore size was further slightly increased to 1.3 μm (which was same as that of the neat membrane). An increased average pore diameter led to an increase in the flux performance [36], justifying that MD applied with the A2 and A3 membranes had the highest flux performance compared to the other samples. In the literature, the pore size distribution of commercial MD membranes generally lies between 0.2 μm and 1 μm as the increase in the maximum pore size greatly decreases the LEP, leading to serious wetting problems [3,6]. Narrowing the range of the pore diameter greatly improves the wetting resistance as the LEPs of A2

and A3 were much higher than that of the neat membrane. The other factor regarding the improvement of the wetting resistance was the evolution of the crystalline structure in the micro-view, which was fully discussed in last two sections. The heat-pressing process turned the amorphous state of the PVDF into crystalline phases, which had much higher thermal and mechanical stability [30]; the annealing process helped some of the β - and amorphous-phase PVDF get converted into the α phase, which had higher hydrophobicity owing to its non-polar structure. Both factors contributed to A2's high wetting resistance in the MD process even though it had the highest average pore size (but a narrower pore size distribution). A high average pore size led to a high flux performance, improving the permeation efficiency of the MD. A3 had a nearly identical pore diameter distribution as A2; therefore, annealing for two days was sufficient for the improvement of the pore diameter distributions.

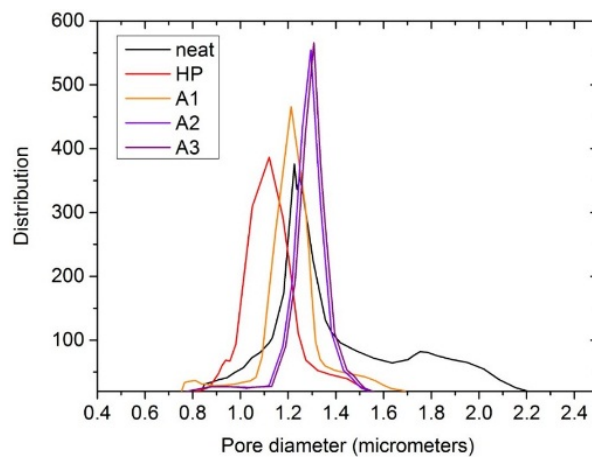


Figure 5. Pore diameter distribution of as-spun and post-treated electrospun membranes.

The porosities of the neat and thermal-treated membranes did not have significant differences. The porosities of the neat, HP, A1, A2, A3 membranes were 91%, 86%, 86%, 87% and 87%, respectively, somehow following the trend of the contact angle. However, their differences were too minimal to affect the MD flux performance.

3.4.2. LEP and Contact Angle

A comparison of the membrane properties of the LEP, contact angle and pore size between the as-spun and post-treated membranes was investigated. Consistent with the previous study [24], Figure 6 shows that the LEP of the neat membrane was the lowest, contributing to the rapid wetting in DCMD. After the membrane was heat-pressed, the LEP increased dramatically from 73 kPa to 91 kPa owing to the vastly decreased average pore diameter and increased crystallinity, although the contact angle decreased from 153° to 142° owing to the reduced roughness [24]. Annealing the HP membranes does not result in a significant change of the LEP as the effect of the increased pore sizes is offset by the increase in the hydrophobicity of the membranes, indicated by the increased contact angle. A2 shares a nearly identical LEP as the HP while it had the highest pore size ($1.3 \mu\text{m}$) owing to a greatly increased contact angle of 147° . Two days of annealing is proved to be sufficient for the improvement of the properties as A3 shares a nearly identical LEP, contact angle and average pore diameter as A2. It is worth mentioning that support layers had minimal effects on the LEP owing to the hydrophilicity and large pore size. The introduction of support layers into the DCMD test mainly aimed to improve the mechanical strength of the electrospun membranes. However, the use of the support layer increased the mass transfer resistance and caused additional temperature polarization, which requires further study [6].

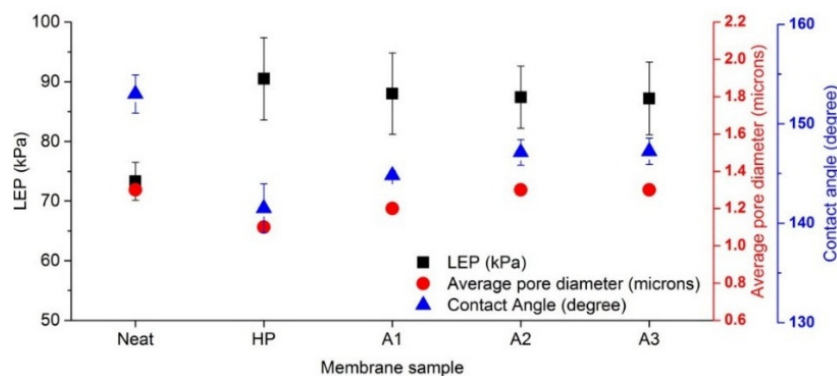


Figure 6. Comparison of LEP (liquid entry pressure), contact angle and average pore diameter of as-spun, heat-pressed, and annealed membranes.

4. Conclusions

In the present study, we successfully fabricated electrospun nanofiber membranes and they were modified by post-treatments such as heat-pressing and annealing. Especially, the effects of annealing on the improvement of the MD flux performance were investigated. Based on the results, it was found that the sufficiently annealed electrospun membranes had a slightly increased average pore size, which contributed to their much higher flux in the DCMD compared to the other membrane samples. An average flux of 35 LMH could be achieved for annealed membranes while an average flux of 20 LMH was obtained by using commercial PVDF membranes in the same DCMD setup during 10 h of operation. It was found that the increase in the α phase of PVDF led to the increase in the hydrophobicity of the membrane, so the high LEP after heat-pressing remained unchanged, although the average pore diameter increased. The other key factor in terms of the wetting resistance was the greatly narrowed pore size distribution as the membranes annealed for two and three days had the narrowest distribution among all the samples. Therefore, the higher average pore size of the annealed electrospun membranes contributed to the improvement of the flux performance while its negative effect on the LEP was offset by the increase in the hydrophobicity, preventing wetting issues. In summary, along with heat-pressing, the annealing technique is recommended for electrospun nanofiber membranes to improve their characteristics such as LEP, contact angle and pore size, which is key for a better permeation and rejection performance of MD for desalination. The use of nanofiber membranes with proper tuning of the material, process and post-treatment parameters to obtain near-ideal MD membranes with high performance efficiency can potentially accelerate their industrial applications.

Acknowledgments: This research was supported by a grant (16IFIP-B065893-04) from the Industrial Facilities & Infrastructure Research Program funded by the Ministry of Land, Infrastructure and Transport of the Korean government. The authors also acknowledge the grant from the ARC Future Fellowship (FT140101208) and the UTS FEIT Blue Sky Research Fund.

Author Contributions: M.Y., L.D.T. and H.K.S. conceived and designed the experiments; M.Y., Y.C.W. and C.C. performed the experiments, helped with data acquisition and prepared the figures; M.Y., Y.C.W., L.D.T. and H.K.S. analyzed the data; M.Y., Y.C.W. and L.D.T. wrote the paper; and H.K.S. and L.D.T. supervised and approved the research plan.

Conflicts of Interest: The authors declare no conflict of interest.

References

1. Efome, J.E.; Rana, D.; Matsuura, T.; Lan, C.Q. Enhanced performance of pvdf nanocomposite membrane by nanofiber coating: A membrane for sustainable desalination through md. *Water Res.* **2016**, *89*, 39–49. [[CrossRef](#)] [[PubMed](#)]

2. Drioli, E.; Ali, A.; Macedonio, F. Membrane distillation: Recent developments and perspectives. *Desalination* **2015**, *356*, 56–84. [[CrossRef](#)]
3. Camacho, L.M.; Dumée, L.; Zhang, J.; Li, J.-D.; Duke, M.; Gomez, J.; Gray, S. Advances in membrane distillation for water desalination and purification applications. *Water* **2013**, *5*, 94–196. [[CrossRef](#)]
4. Cho, D.-W.; Song, H.; Yoon, K.; Kim, S.; Han, J.; Cho, J. Treatment of simulated coalbed methane produced water using direct contact membrane distillation. *Water* **2016**, *8*, 194. [[CrossRef](#)]
5. Alkhudhiri, A.; Darwish, N.; Hilal, N. Membrane distillation: A comprehensive review. *Desalination* **2012**, *287*, 2–18. [[CrossRef](#)]
6. Eykens, L.; de Sitter, K.; Dotremont, C.; Pinoy, L.; van der Bruggen, B. How to optimize the membrane properties for membrane distillation: A review. *Ind. Eng. Chem. Res.* **2016**, *55*, 9333–9343. [[CrossRef](#)]
7. Guillen-Burrieza, E.; Mavukkandy, M.O.; Bilad, M.R.; Arafat, H.A. Understanding wetting phenomena in membrane distillation and how operational parameters can affect it. *J. Membr. Sci.* **2016**, *515*, 163–174. [[CrossRef](#)]
8. Ke, H.; Feldman, E.; Guzman, P.; Cole, J.; Wei, Q.; Chu, B.; Alkhudhiri, A.; Alrasheed, R.; Hsiao, B.S. Electrospun polystyrene nanofibrous membranes for direct contact membrane distillation. *J. Membr. Sci.* **2016**, *515*, 86–97. [[CrossRef](#)]
9. Woo, Y.C.; Tijjing, L.D.; Park, M.J.; Yao, M.; Choi, J.-S.; Lee, S.; Kim, S.-H.; An, K.-J.; Shon, H.K. Electrospun dual-layer nonwoven membrane for desalination by air gap membrane distillation. *Desalination* **2017**, *403*, 187–198. [[CrossRef](#)]
10. Ma, M.; Hill, R.M.; Lowery, J.L.; Fridrikh, S.V.; Rutledge, G.C. Electrospun poly(styrene-block-dimethylsiloxane) block copolymer fibers exhibiting superhydrophobicity. *Langmuir* **2005**, *21*, 5549–5554. [[CrossRef](#)] [[PubMed](#)]
11. Zhang, J.; Li, J.-D.; Gray, S. Effect of applied pressure on performance of ptfе membrane in dcmd. *J. Membr. Sci.* **2011**, *369*, 514–525. [[CrossRef](#)]
12. Woo, Y.C.; Kim, Y.; Shim, W.-G.; Tijjing, L.D.; Yao, M.; Nghiem, L.D.; Choi, J.-S.; Kim, S.-H.; Shon, H.K. Graphene/PVDF flat-sheet membrane for the treatment of ro brine from coal seam gas produced water by air gap membrane distillation. *J. Membr. Sci.* **2016**, *513*, 74–84. [[CrossRef](#)]
13. Prince, J.; Rana, D.; Singh, G.; Matsuura, T.; Kai, T.J.; Shanmugasundaram, T. Effect of hydrophobic surface modifying macromolecules on differently produced pvdf membranes for direct contact membrane distillation. *Chem. Eng. J.* **2014**, *242*, 387–396. [[CrossRef](#)]
14. Hwang, H.J.; He, K.; Gray, S.; Zhang, J.; Moon, I.S. Direct contact membrane distillation (DCMD): Experimental study on the commercial ptfе membrane and modeling. *J. Membr. Sci.* **2011**, *371*, 90–98. [[CrossRef](#)]
15. Tijjing, L.D.; Choi, J.-S.; Lee, S.; Kim, S.-H.; Shon, H.K. Recent progress of membrane distillation using electrospun nanofibrous membrane. *J. Membr. Sci.* **2014**, *453*, 435–462. [[CrossRef](#)]
16. Liao, Y.; Wang, R.; Fane, A.G. Fabrication of bioinspired composite nanofiber membranes with robust superhydrophobicity for direct contact membrane distillation. *Environ. Sci. Technol.* **2014**, *48*, 6335–6341. [[CrossRef](#)] [[PubMed](#)]
17. Feng, C.; Khulbe, K.C.; Matsuura, T.; Tabe, S.; Ismail, A.F. Preparation and characterization of electro-spun nanofiber membranes and their possible applications in water treatment. *Sep. Purif. Technol.* **2013**, *102*, 118–135. [[CrossRef](#)]
18. Ahmed, F.E.; Lalia, B.S.; Hashaikeh, R. A review on electrospinning for membrane fabrication: Challenges and applications. *Desalination* **2015**, *356*, 15–30. [[CrossRef](#)]
19. Prince, J.; Rana, D.; Matsuura, T.; Ayyanar, N.; Shanmugasundaram, T.; Singh, G. Nanofiber based triple layer hydro-philic/-phobic membrane-a solution for pore wetting in membrane distillation. *Sci. Rep.* **2014**, *4*, 6949. [[CrossRef](#)] [[PubMed](#)]
20. Lee, E.-J.; An, A.K.; He, T.; Woo, Y.C.; Shon, H.K. Electrospun nanofiber membranes incorporating fluorosilane-coated TiO₂ nanocomposite for direct contact membrane distillation. *J. Membr. Sci.* **2016**, *520*, 145–154. [[CrossRef](#)]
21. Tijjing, L.D.; Woo, Y.C.; Shim, W.-G.; He, T.; Choi, J.-S.; Kim, S.-H.; Shon, H.K. Superhydrophobic nanofiber membrane containing carbon nanotubes for high-performance direct contact membrane distillation. *J. Membr. Sci.* **2016**, *502*, 158–170. [[CrossRef](#)]

22. Ren, L.-F.; Xia, F.; Shao, J.; Zhang, X.; Li, J. Experimental investigation of the effect of electrospinning parameters on properties of superhydrophobic PDMS/PMMA membrane and its application in membrane distillation. *Desalination* **2017**, *404*, 155–166. [[CrossRef](#)]
23. An, A.K.; Guo, J.; Lee, E.-J.; Jeong, S.; Zhao, Y.; Wang, Z.; Leiknes, T. PDMS/PVDF hybrid electrospun membrane with superhydrophobic property and drop impact dynamics for dyeing wastewater treatment using membrane distillation. *J. Membr. Sci.* **2017**, *525*, 57–67. [[CrossRef](#)]
24. Yao, M.; Woo, Y.C.; Tijing, L.D.; Shim, W.-G.; Choi, J.-S.; Kim, S.-H.; Shon, H.K. Effect of heat-press conditions on electrospun membranes for desalination by direct contact membrane distillation. *Desalination* **2016**, *378*, 80–91. [[CrossRef](#)]
25. Na, H.; Zhao, Y.; Zhao, C.; Zhao, C.; Yuan, X. Effect of hot-press on electrospun poly(vinylidene fluoride) membranes. *Polym. Eng. Sci.* **2008**, *48*, 934–940. [[CrossRef](#)]
26. Tijing, L.D.; Woo, Y.C.; Johir, M.A.H.; Choi, J.-S.; Shon, H.K. A novel dual-layer bicomponent electrospun nanofibrous membrane for desalination by direct contact membrane distillation. *Chem. Eng. J.* **2014**, *256*, 155–159. [[CrossRef](#)]
27. Liao, Y.; Wang, R.; Tian, M.; Qiu, C.; Fane, A.G. Fabrication of polyvinylidene fluoride (PVDF) nanofiber membranes by electro-spinning for direct contact membrane distillation. *J. Membr. Sci.* **2013**, *425–426*, 30–39. [[CrossRef](#)]
28. Lalia, B.S.; Guillen-Burrieza, E.; Arafat, H.A.; Hashaikeh, R. Fabrication and characterization of polyvinylidene fluoride-co-hexafluoropropylene (PVDF-HFP) electrospun membranes for direct contact membrane distillation. *J. Membr. Sci.* **2013**, *428*, 104–115. [[CrossRef](#)]
29. Du, C.-H.; Zhu, B.-K.; Xu, Y.-Y. The effects of quenching on the phase structure of vinylidene fluoride segments in PVDF-HFP copolymer and PVDF-HFP/PMMA blends. *J. Mater. Sci.* **2006**, *41*, 417–421. [[CrossRef](#)]
30. Liu, J.; Lu, X.; Wu, C. Effect of preparation methods on crystallization behavior and tensile strength of poly(vinylidene fluoride) membranes. *Membranes* **2013**, *3*, 389–405. [[CrossRef](#)] [[PubMed](#)]
31. Salimi, A.; Yousefi, A. Analysis method: Ftir studies of β -phase crystal formation in stretched PVDF films. *Polym. Test.* **2003**, *22*, 699–704. [[CrossRef](#)]
32. Esterly, D.M. Manufacturing of Poly(vinylidene fluoride) and Evaluation of Its Mechanical Properties. Master's Thesis, Virginia Polytechnic Institute and State University, Blacksburg, CA, USA, 2002.
33. Tiwari, V.; Srivastava, G. Effect of thermal processing conditions on the structure and dielectric properties of pvdf films. *J. Polym. Res.* **2014**, *21*, 1–8. [[CrossRef](#)]
34. Aqeel, S.M.; Wang, Z.; Than, L.; Sreenivasulu, G.; Zeng, X. Poly(vinylidene fluoride)/poly(acrylonitrile)-based superior hydrophobic piezoelectric solid derived by aligned carbon nanotubes in electrospinning: Fabrication, phase conversion and surface energy. *RSC Adv.* **2015**, *5*, 76383–76391. [[CrossRef](#)] [[PubMed](#)]
35. Saffarini, R.B.; Mansoor, B.; Thomas, R.; Arafat, H.A. Effect of temperature-dependent microstructure evolution on pore wetting in ptfе membranes under membrane distillation conditions. *J. Membr. Sci.* **2013**, *429*, 282–294.
36. Manawi, Y.M.; Khraisheh, M.; Fard, A.K.; Benyahia, F.; Adham, S. Effect of operational parameters on distillate flux in direct contact membrane distillation (DCMD): Comparison between experimental and model predicted performance. *Desalination* **2014**, *336*, 110–120. [[CrossRef](#)]

